Korean J. Chem. Eng., 35(11), 2303-2312 (2018)
DOI: 10.1007/s11814-018-0130-9

pISSN: 0256-1115
eISSN: 1975-7220

Pretreatment of low-grade poly(ethylene terephthalate) waste for effective depolymerization to monomers

Yunsu Kim and Do Hyun Kim†

Department of Chemical & Biomolecular Engineering, KAIST, 291 Daehak-ro, Yuseong-gu, Daejeon 34141, Korea

(*Received 16 April 2018 • accepted 26 July 2018*)

Abstract–Pretreatment process of silica-coated PET fabrics, a major low-grade PET waste, was developed using the reaction with NaOH solution. By destroying the structure of silica coating layer, impurities such as silica and pigment dyes could be removed. The removal of impurity was confirmed by X-ray photoelectron spectroscopy (XPS), scanning electron microscopy (SEM), and energy dispersive X-ray spectroscopy (EDX). The pretreated PET fabric samples were used for depolymerization into its monomer, bis(2-hydroxylethyl) terephthalate (BHET), by glycolysis with ethylene glycol (EG), and zinc acetate (ZnAc) catalyst. The quality of BHET was confirmed by DSC, TGA, HPLC and NMR analyses. The highest BHET yield of 89.23% was obtained from pretreated PET fabrics, while glycolysis with raw PET fabric yielded 85.43%. The BHET yield from untreated silica-coated PET fabrics was 60.39%. The pretreatment process enhances the monomer yield by the removal of impurity and also improves the quality of the monomer.

Keywords: Pretreatment, Low-grade PET Wastes, Glycolysis, Zinc Acetate, BHET

INTRODUCTION

Poly(ethylene terephthalate) (PET) is one of the most widely used thermoplastic polymers in our daily lives. Due to its excellent thermophysical properties and relatively low material cost, the total PET consumption exceeds 50 million tons per year worldwide and the demand is still increasing [1]. Polyester fibers and bottles are the main PET commercial products in the world, representing 63.5% and 30.3%, respectively [2]. The increase of PET consumption causes serious pollution and waste management problems [3]. PET is one of the most recycled materials, second to aluminum, but only clean and transparent PET bottles are recycled to produce commercial products [4].

There are physical and chemical methods to recycle PET waste materials. Physical recycling simply reprocesses PET waste by mechanical means to make commercial products with inferior properties. Chemical recycling involves degradation of PET to its monomers by depolymerization process, and the produced monomers can be used in various processes to make commercial PET products such as film, polyester resin, polyurethane, and dyestuff [5-9]. Since it produces raw materials for various commercial products, chemical recycling is acceptable to the principles of sustainable development [10]. Many researchers have studied PET depolymerization process to improve the yield, and selectivity of PET monomers, but still there is an issue associated with impurity in PET waste materials [11-13]. The impurity in PET waste can reduce the monomer yield, catalytic activity and the product quality. A PET waste materials with a high level of impurity including mixture of organic or inorganic materials such as coating layers, synthetic binders, dyes, and dusts, can be classified as low-grade PET waste. To recycle the low-grade PET waste to PET products with high quality, the impurity must be removed before depolymerization. However, there have been only a few attempts for the removal of impurity [14]. We have developed a new strategy to eliminate impurity efficiently from the low-grade PET waste.

The silica-coated PET fabrics, commonly used for outdoor advertisement, are the main low-grade PET waste from digital textile printing (DTP) industry [15,16]. Hydrophilic fumed silica is coated to the surface of PET fabrics. The nanosized individual silica particles are fused together to form aggregates and further up to agglomerate by hydrogen bonding and electrostatic interactions [17-19]. The coating layer with fused aggregates and agglomerates has network porosity to form spongy-like interparticle voids and capillaries of the coating layer where the water-dye droplets of the ink are absorbed [20-22]. These porous structures provide fast ink absorption, excellent dye binding property and outstanding structure stability.

The domestic disposal rate of silica-coated PET fabric waste has been continuously increasing and the annual disposal rate is expected as 10,000 tons per year. This causes serious environmental problems since the fabric waste cannot be recycled due to high level of impurity. The pretreatment process of silica-coated PET fabric waste is not commercially developed yet to remove surface impurities from the fabric for recycling.

The key to removing the impurity from silica-coated PET fabrics is to destroy the structure of silica coating layer. Strong alkali such as sodium hydroxide (NaOH), potassium hydroxide (KOH) solutions can dissolve silica compounds [23-25]. Pretreatment of silica-coated PET fabrics with NaOH solution can destroy the silica coating layer by dissolving silica particles, allowing the removal of dyes and other impurities easily from the fabrics, thus improving the monomer yield and quality. Pretreatment also helps the depolymerization process because NaOH treatment attacks and

---

† To whom correspondence should be addressed.
E-mail: DoHyun.Kim@kaist.ac.kr

partially cleaves the PET chain with OH^- by alkaline hydrolysis [26,27].

The main PET depolymerization reactions commercially viable are methanolysis and glycolysis [28,29]. In methanolysis, PET is depolymerized to dimethyl terephthalate (DMT) by methanol. Main disadvantage of this method is the high operation cost associated with separation and refining of the DMT monomers. On the other hand, glycolysis is the simplest, oldest, and least capital intensive process that produces bis(2-hydroxyethyl) terephthalate (BHET) by reaction with ethylene glycol (EG). Numerous researches have been conducted to study the PET glycolysis due to such great advantages.

In this study, we developed a novel pretreatment strategy to remove impurity from silica-coated PET fabrics by the alkali reaction with NaOH solution. To verify the effectiveness of pretreatment, the pretreated PET fabrics were depolymerized by EG glycolysis with zinc acetate (ZnAC) catalyst.

EXPERIMENTAL

1. Materials

Commercial silica-coated PET fabrics and standard PET fabrics were purchased from Jin Kwang Chemical Co. For the extraction of fumed silica from silica-coated PET fabrics, toluene was purchased from Sigma Aldrich. For comparison of properties of extracted fumed silica, commercial fumed silica (Aerosil OX 50) was purchased from Evonik. For the solubility of silica in alkaline solution and the pretreatment of silica-coated PET fabrics, 95% sodium hydroxide (NaOH), and 85% potassium hydroxide (KOH) were purchased from Junsei Chemical. For the neutralization of residual NaOH in fabric samples, 35% hydrochloric acid (HCl) was purchased from Junsei Chemical. The anhydrous ethylene glycol (EG), zinc acetate (ZnAc), standard BHET for characterization, and dimethylsulfoxide (DMSO-d6) were purchased from Sigma Aldrich.

2. Extraction of Fumed Silica from Silica-coated PET Fabrics

To investigate the characteristics of fumed silica used for silica-coated PET fabrics, coating of commercial silica-coated PET fabrics was removed from the fabric samples. The coating debris was immersed in toluene solution under sonication to dissolve organic components. After sonication, distilled water was added to the solution. The resulting two-phase system was stirred to transfer the fumed silica to the aqueous phase. The aqueous phase was separated from the toluene phase and distillation was done to remove water and residual toluene from the silica component. The recovered fumed silica was dried at 70 °C for 24 hours.

3. Solubility of Fumed Silica in Alkaline Solution

To test solubility of fumed silica in alkaline solution, NaOH and KOH solutions were prepared with molar concentration of 1.25 mol/L. 0.2 g fumed silica was reacted with 25 mL alkaline solutions at 60 °C for various dissolution time. The solutions were quickly cooled by quenching to stop the dissolution. The conductivity of the solutions was measured by conductivity meter (Orion Versa Star, Thermo Scientific) to compare the dissolution rate of fumed silica in NaOH and KOH solutions.

4. Pretreatment of Silica-coated PET Fabrics

Silica-coated PET fabrics to be tested were cut into 10 cm×10 cm pieces, and the samples were reacted with 10%, 7.5%, 5% NaOH solutions at 95 °C, 85 °C, 75 °C, 65 °C for various reaction time. The optimal liquor ratio of the fabric samples to NaOH solution was also investigated. To check recyclability of NaOH solution, the fabric samples were reacted with the same NaOH solution several times and the Si atomic percentage on pretreated fabric samples was investigated by X-ray photoelectron spectroscopy (XPS, Sigma Probe, Thermo VG Scientific). After the NaOH treatment, the fabric samples were rinsed with 1% HCl solution to neutralize the residual OH^- ions on the samples, and washed with distilled water several times. Pretreated samples were dried in vacuum oven at 70 °C for 10 minutes.

5. Glycolysis of PET Fabric Samples

The optimal glycolysis reaction conditions with zinc acetate (ZnAc) catalyst system is based on the previous work with minor modification [30]. The glycolysis reaction was carried out in 500 mL round glass type reactor at 196 °C for three hours under reflux in a nitrogen atmosphere. 9 g PET fabric samples (raw PET fabric, black silica-coated PET fabric, and pretreated PET fabric) were reacted with 45 g EG, and 0.09 g ZnAc catalyst. After the glycolysis reaction, the unreacted PET components were separated from the glycolysis reaction products by filtration through iron mesh. The unreacted samples were rinsed with distilled water, and the wash solution was added to the glycolysis reaction product. For quantitative determination of the BHET, boiling water was added to the glycolysis reaction products, and the mixture was stirred under constant temperature of 85 °C for 5 minutes. Hot mixture solution was filtered (first filtration) immediately using Whatman (pore size=11 μm) filter paper. The filter-cake was dried under vacuum at 40 °C, and then weighed as the oligomer fraction. Immediately after the first filtration, floccules in the filtrate started to be formed. The filtrate was kept at 4 °C for 24 hours, and white crystals of BHET flakes were formed. The white crystalline BHET flakes were filtered (second filtration), dried under vacuum at 40 °C, and weighted as the BHET fraction. The yield of BHET was calculated by the following equation:

$$\text{Yield of BHET (mol\%)} = (\text{moles of BHET produced}/\text{moles of PET repeat units})\times 100 \quad (1)$$

6. Characterization

The morphology and particle size of extracted fumed silica and commercial fumed silica was investigated with field emission transmission electron microscope (Talos F200X, FEI). The aggregate size of extracted fumed silica and commercial fumed silica was determined with particle size analyzer (ELS-Z2, Otsukael). The surface charge of the extracted fumed silica was investigated by measuring zeta potential with zeta potential analyzer (ELS-Z2, Otsukael). The silanol group of extracted fumed silica from silica-coated PET fabrics was confirmed by FTIR (Nicolet iS50, Thermo Fisher Scientific Instrument).

The surface of silica-coated PET fabric and pretreated PET fabric samples was analyzed by field emission scanning electron microscope (FE-SEM; Magellan 400), which was coupled with energy dispersive X-ray spectroscopy (EDX) for elemental composition analysis of the microscopic surface. The Si atomic percentage of pretreated PET fabric samples was investigated with XPS to study the effect of temperature, NaOH concentration, and NaOH reaction time.

The viscosity-average molecular weight of virgin PET fabric and pretreated PET fabric samples were determined by dilute solution viscometry to investigate the effect of NaOH treatment on fabric samples. The intrinsic viscosity of dilute PET solutions in 60/40 (w/w) phenol/1,1,2,2-tetrachloroethane were measured in a Type 1C Ubbelohde viscometer at 25 °C. From the intrinsic viscosity, the number average molecular weight can be calculated from the following relationship [31]:

$$M_n=(4.31\times10^4)\eta^{1.35} \tag{2}$$

where:
M_n=number average molecular weight;
η=intrinsic viscosity.

The quality of BHET obtained from pretreated PET fabric samples was confirmed by differential scanning calorimeter (DSC; SDT-Q20, TA Instruments), thermogravimetric analyzer (TGA; TG209 F1 Libra, NETZSCH), high-performance liquid chromatography (HPLC; Waters 600 series, Waters) and nuclear magnetic resonance spectroscopy (Agilent 400 NB, Agilent). To check the melting point of the BHET, DSC was carried out with a heating rate of 10 °C/min under nitrogen gas in the range 25-225 °C. The weight loss of BHET sample during temperature ramping from 30 °C to 700 °C was measured under nitrogen flow at a rate of 10 mL/min and at a heating rate of 10 °C/min. In HPLC, UV detector wavelength was set at 254 nm and a reverse-phase Zorbax-C8 column was used to analyze the samples. The samples for HPLC analysis were prepared by dissolving the BHET samples in THF. The injection volume was 20 μL and the column temperature was 25 °C. The mobile phase was 50 : 50 (v/v) THF/H_2O solution at the flow rate of 1.0 mL/min. The chemical structure of BHET was analyzed by ^{1}H-NMR, and ^{13}C-NMR operating at 500 MHz. The NMR spectra were obtained using DMSO-d6 solvent.

RESULTS AND DISCUSSION

1. Characteristics of Fumed Silica

The fumed silica was extracted from silica-coated PET fabrics to investigate its characteristics. Fig. 1 shows TEM images of extracted fumed silica and commercial fumed silica. In both extracted and commercial samples, nanosized silica particles were clustered to form aggregate with 3D network. According to Table 1, average

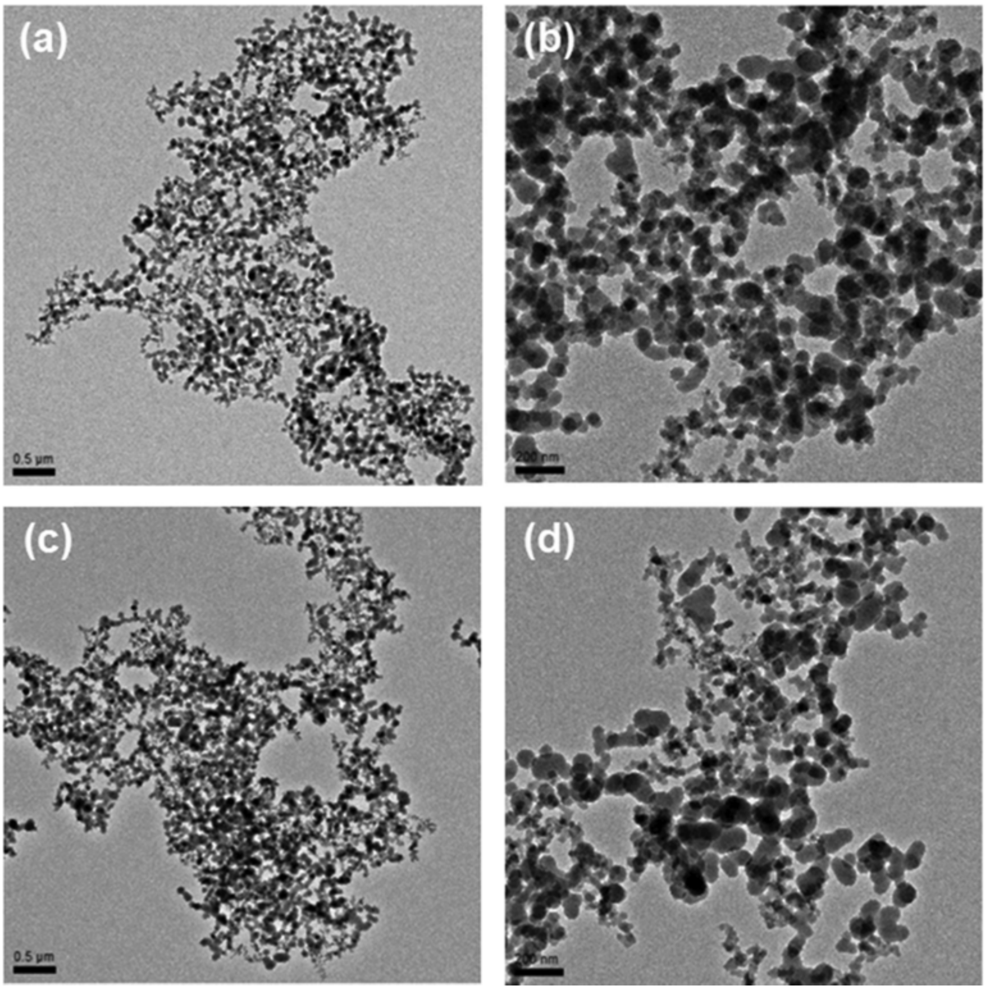

Fig. 1. TEM images of (a) extracted fumed silica, (b) magnified extracted fumed silica, (c) commercial fumed silica, (d) magnified commercial fumed silica.

Table 1. Average particle size, average aggregate size and zeta potential of extracted fumed silica and commercial fumed silica

Sample name	Average particle size (nm)	Average aggregate size (nm)	Zeta potential (mV)
Extracted fumed silica	36	317.7	−39.77
Commercial fumed silica	42	328.8	−40.19

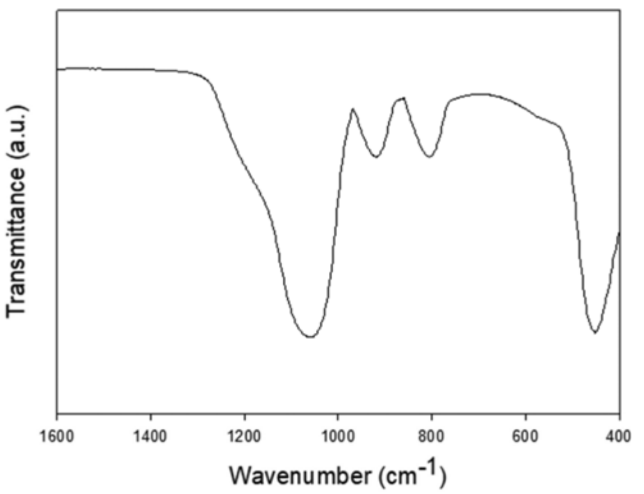

Fig. 2. FTIR scan of extracted fumed silica from silica-coated PET fabric.

particle size of extracted and commercial fumed silica was 36 and 42 nm, and average aggregate size 317 and 328 nm, respectively. It was reported that 5-50 nm silica particles were fused to form 100-500 nm aggregate by hydrogen bonding and electrostatic interactions [17]. The zeta potential of extracted fumed silica and commercial fumed silica was −39.77 and −40.19, which shows hydrophilic property. Fig. 2 shows FTIR scan of extracted fumed silica from silica-coated PET fabric. The Si-O-Si asymmetric stretching at 1,050 cm^{-1}, the O-Si-O bending mode at 450 cm^{-1}, and the Si-O-Si symmetric stretching at 810 cm^{-1} were observed with similar results from previous studies [32-34]. The peak related to silanol group (Si-OH) reported previously [33] was also observed at 920 cm^{-1}. It was reported that silica particle forms hydrophilic characteristic due to silanol group [17].

2. Solubility of Fumed Silica in Alkaline Solution

The dissolution of fumed silica in NaOH and KOH solution was investigated by measuring the conductivity of sample solutions. Fig. 3(a) shows conductivity of NaOH and KOH solutions with fumed silica at 60 °C with various dissolution time. The conductivity of both NaOH and KOH solutions was decreased similarly with the same molar concentration of 1.25 mol/L. This shows that OH$^-$ rather than Na$^+$ or K$^+$ ions is responsible for the solubility of fumed silica in alkaline solution. Based on these results, the dissolution rate of fumed silica in NaOH and KOH solutions was evaluated in Fig. 3(b), and the results show the similar patterns of the dissolution rate. The dissolution of silica in alkaline solution has several reactions simultaneously in aqueous medium and some reactions are reported as [35]:

$$SiO_{2(sd)}+2OH^- \rightarrow H_2SiO_4^{2-} \quad (3)$$

$$2SiO_{2(sd)}+2OH^- \rightarrow H_2Si_2O_6^{2-} \quad (4)$$

$$3SiO_{2(sd)}+2OH^- \rightarrow H_2Si_3O_8^{2-} \quad (5)$$

The above reactions indicate that there are a variety of silicate anions present after reaction of silica with NaOH solution. Since several reactions take place for silica dissolution in alkaline solution, the dissolution rate is not constant as shown in Fig. 3(b).

3. Pretreatment of Silica-coated PET Fabrics

The silica-coated PET fabrics were reacted with 10%, 7.5%, 5% NaOH solutions at 95 °C, 85 °C, 75 °C, 65 °C for various reaction time and the results are shown in Fig. 4. Si atomic percentage on pretreated PET fabric samples was gradually reduced as NaOH reaction time increased. It was found that slower NaOH reaction rate happens with concentration and temperature decrease. The reaction rate is not constant since the dissolution of silica in NaOH

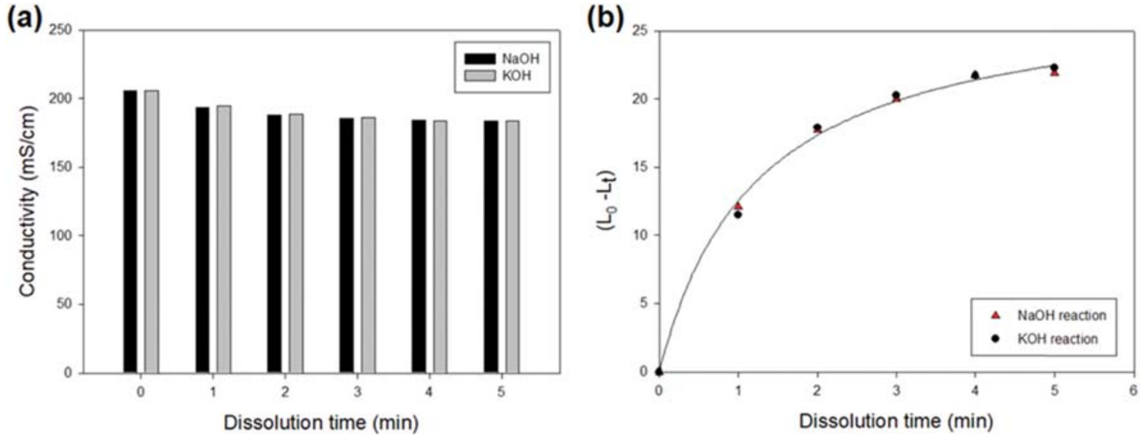

Fig. 3. (a) Conductivity of NaOH and KOH solution with fumed silica at 60 °C with various dissolution time. (b) Comparison of dissolution rate of fumed silica in NaOH and KOH solutions.

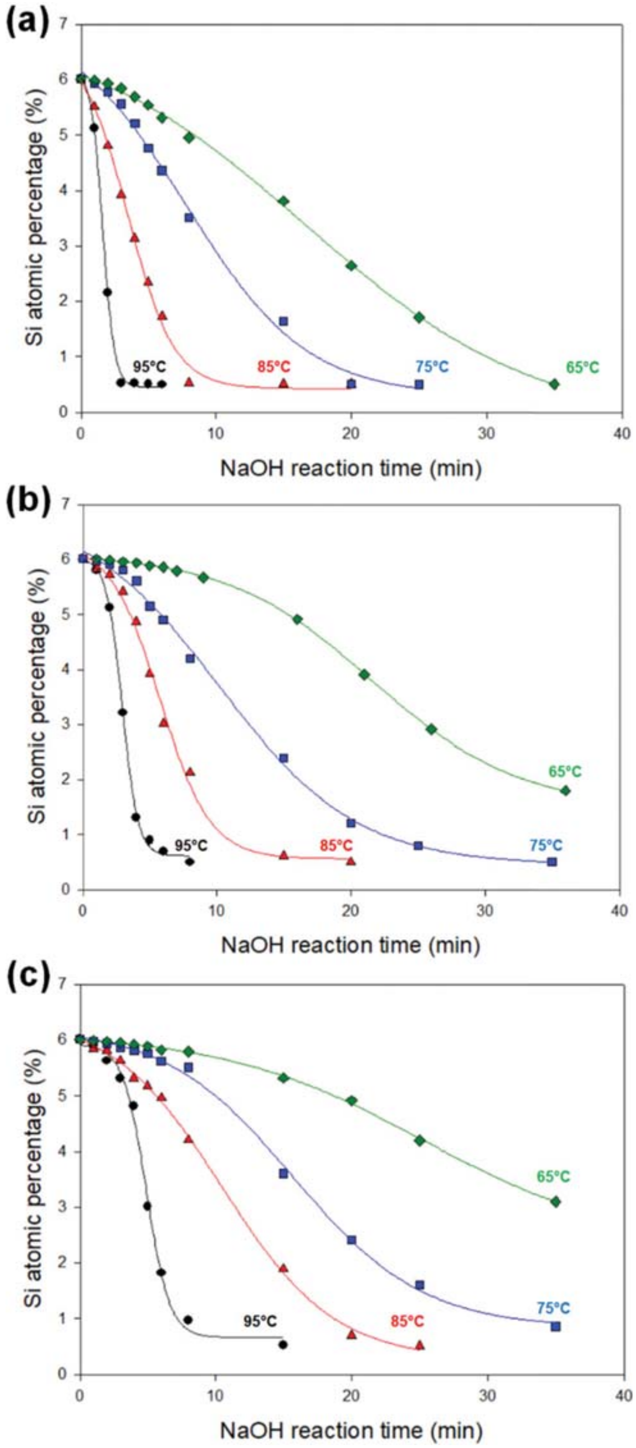

Fig. 4. NaOH reaction rate of silica-coated PET fabric at different reaction temperature with (a) 10% NaOH solution, (b) 7.5% NaOH solution, (c) 5% NaOH solution.

solution has multiple reactions [24,35]. Based on 5% NaOH solution at 85 °C, the optimal reaction time was 25 minutes.

NaOH reaction with different liquor ratio of silica-coated PET fabric samples to NaOH solution was also investigated to find the optimal point. Fig. 5 shows effect of liquor ratio of the fabric samples to NaOH solution on Si atomic percentage of pretreated PET fabric. As the liquor ratio was decreased from 1 : 10 to 1 : 8, the Si atomic percentage was remained constant as 0.5%. The Si atomic percentage started to increase from liquor ratio of 1 : 7, indicating that there was not sufficient amounts of NaOH solution to react the whole fabric samples.

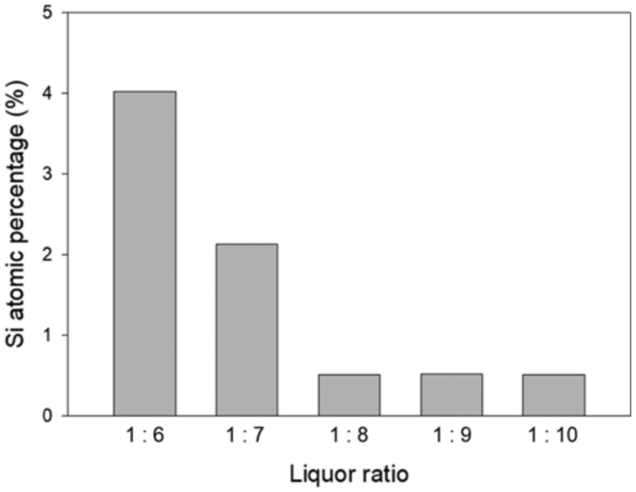

Fig. 5. Effect of liquor ratio of silica-coated PET fabric samples to NaOH solution on Si atomic percentage of pretreated PET fabric.

The surface morphologies of the silica-coated PET fabric and pretreated PET fabric samples were investigated by SEM analysis, and the surface elemental composition was determined by EDX. Fig. 6 shows the SEM images of the silica-coated PET fabric and pretreated PET fabric samples. The top coating surface of the silica-coated PET fabrics has a rigid and spongy-like structure with minor cracks, and some of the PET fibers are exposed (Fig. 6(a) and (b)). The silica aggregates of the coating layer form interparticle voids and capillaries where ink solution permeates into the coating layer (Fig. 6(c)). The ink contains not only the pigment dyes and water but also polymer materials that can assist to bind the dye molecules to the surface of the coating layer. When the silica-coated fabrics are printed and dried out, water is removed and the pigment dyes are bound to the capillary wall of silica aggregates, difficult to be removed from the fabrics. The cross-sectional image shows that the silica aggregates are mostly present on the top surface of the PET fabrics (Fig. 6(d)). By reacting samples with 5% NaOH solution at 85 °C for 25 minutes, the silica coating layer was successfully removed from the PET fabrics (Fig. 6(e) and (f)).

Energy dispersive X-Ray spectroscopy (EDX) was performed on the surface of silica-coated PET fabrics, and pretreated PET fabric samples to investigate the degree of impurity removal. As shown in Table 2, the element content of silicon of silica-coated PET fabrics was 4.5 atomic% initially, and then dramatically decreased to 0.1 atomic% after NaOH treatment. This may imply that NaOH destroys and removes silica coating layer from the silica-coated PET fabrics.

The recyclability of NaOH solution for the pretreatment was investigated. Fig. 7 shows effect of NaOH recycling on Si atomic percentage of pretreated PET fabric samples. As NaOH solution was recycled several times, Si atomic percentage on fabric sample

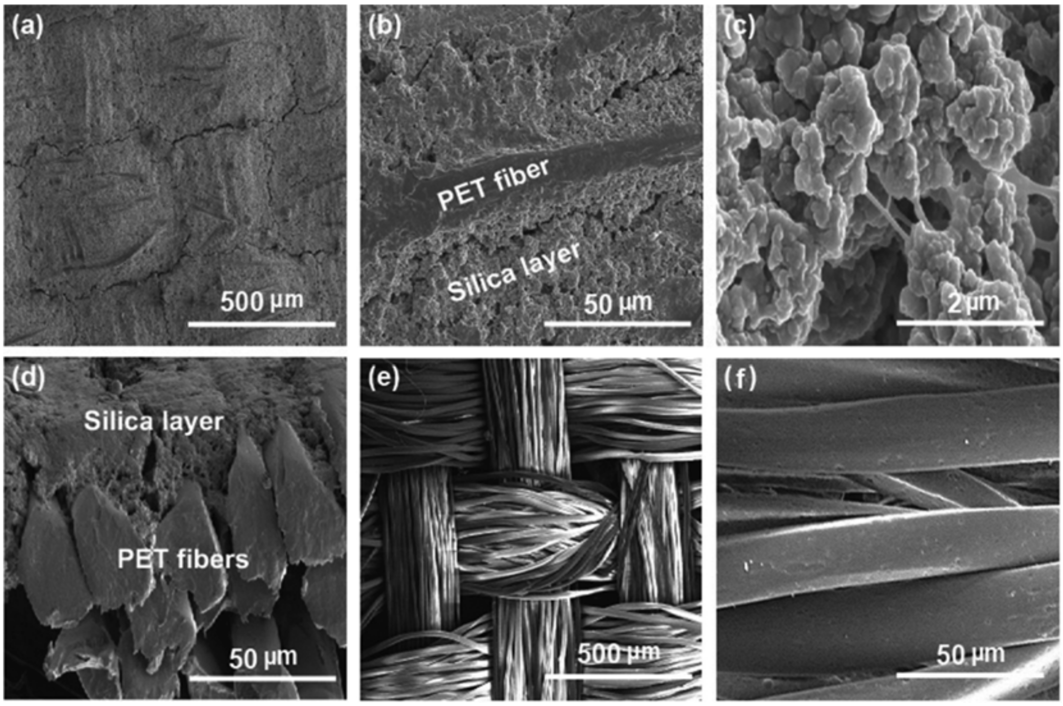

Fig. 6. SEM images of (a) silica-coated PET fabrics, (b) magnified top surface of silica-coated PET fabrics, (c) interparticle voids and capillaries of silica aggregates in coating layer, (d) cross-section of the silica-coated PET fabrics, (e) top surface of pretreated PET fabrics, and (f) top surface of magnified pretreated PET fabrics.

Table 2. EDX results of the surface of silica-coated PET fabrics, and pretreated PET fabrics

Sample		Element content			
		C	O	Al	Si
Silica-coated PET fabrics	wt%	60.6	30	0.1	9.3
	at%	69.6	25.8	0.1	4.5
Pretreated PET fabrics	wt%	62.6	37	0.2	0.2
	at%	69.2	30.6	0.1	0.1

was increased. This happens since the concentration of OH^- ion is gradually reduced by reaction with fumed silica from silica-coated PET fabric samples. Without supplement of NaOH, the solution can be recycled four times as the fabric sample conditions were confirmed by SEM in Fig. 7. By adding additional NaOH to the solution for compensation, NaOH solution could be recycled more than four times.

To check the effect of NaOH treatment on PET samples, the number-average molecular weights of virgin PET fabric and pre-

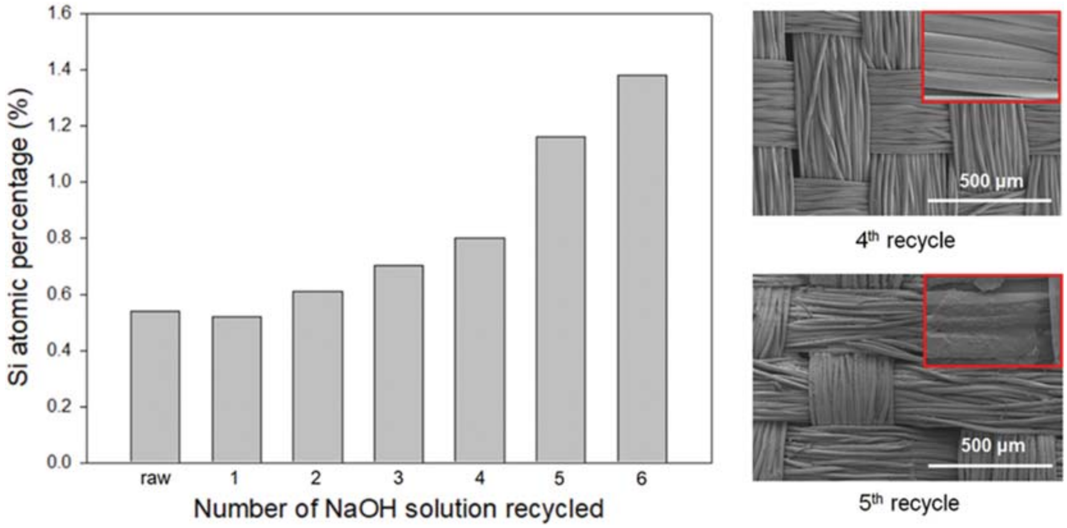

Fig. 7. Effect of NaOH recycling on Si atomic percentage of pretreated PET fabric samples.

Table 3. Intrinsic viscosity and calculated number-average molecular weights of virgin PET fabrics, and pretreated PET fabrics

Sample	Intrinsic viscosity	Number average MW
Virgin PET fabrics	0.58	20,640
Pretreated PET fabrics	0.56	19,684

Table 4. Weight of main glycolysis products and BHET yield of virgin PET fabrics, silica-coated PET fabrics, and pretreated PET fabrics

Sample name	Product type	Weight (g)	Yield (mol%)
Virgin PET fabrics	BHET	10.17	85.43
	Oligomer	0.50	
Silica-coated PET fabrics	BHET	7.19	60.39
	Oligomer	0.80	
Pretreated PET fabrics	BHET	10.62	89.21
	Oligomer	0.37	

treated PET fabric samples were measured by dilute solution viscometry (Table 3). The results show that the molecular weight of PET fabric samples decreased from 20,640 to 19,684, indicating that some of the PET chain of the pretreated samples was partially attacked by NaOH treatment.

4. Glycolysis of PET Fabrics with Zinc Acetate Catalyst

The BHET and oligomers of the glycolysis reaction products of virgin PET fabrics, black silica-coated PET fabrics, and pretreated PET fabrics were extracted and weighed, as shown in Table 4. The yield of BHET generated from virgin PET fabric was 85.43%, similar to results from previous works done by Xi et al. [30]. The BHET yield from black silica-coated PET fabric was 60.39%, and the BHET yield was significantly improved to 89.21% when the black silica-coated PET fabric samples were treated with NaOH solution before glycolysis reaction. One thing to note is that the oligomer content from black silica-coated PET fabrics initially 0.80 g, was also reduced to 0.37 g with NaOH treatment. The presence of silica aggregates could affect the glycolysis reaction by reducing the contact area between the PET and EG. The BHET yield after NaOH treatment was improved since the NaOH could attack and cleave PET chains via alkaline hydrolysis. The resulting shorter PET chains could give the better conversion of PET into BHET.

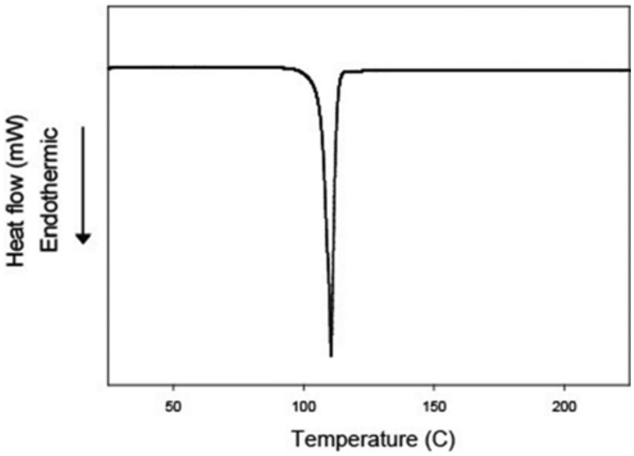

Fig. 8. DSC scan of BHET fraction from pretreated PET fabric samples.

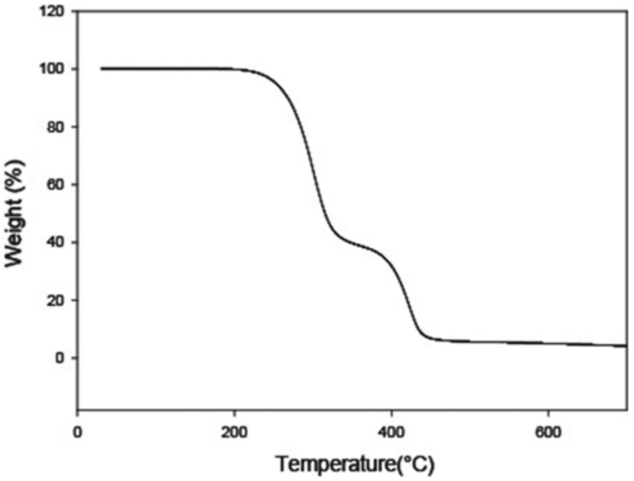

Fig. 9. TGA curve of BHET fraction from pretreated PET fabric samples.

BHET obtained from pretreated PET fabric was characterized by conventional analytical tools. The DSC scan of BHET fraction is shown in Fig. 8. The dominant endothermic peak at 114 °C represents the melting point of BHET monomer, similar to the previous studies [36-38].

The weight loss of BHET sample during temperature ramping from 30 °C to 700 °C is shown in Fig. 9. The first weight loss is about 60% starting from 210 °C due to the thermal decomposition of the BHET sample. The second weight loss is about 30%, beginning from 400 °C. It is due to the thermal decomposition of PET produced by the BHET thermal polymerization during the thermogravimetric analysis measurement. The TGA results agree well with previ-

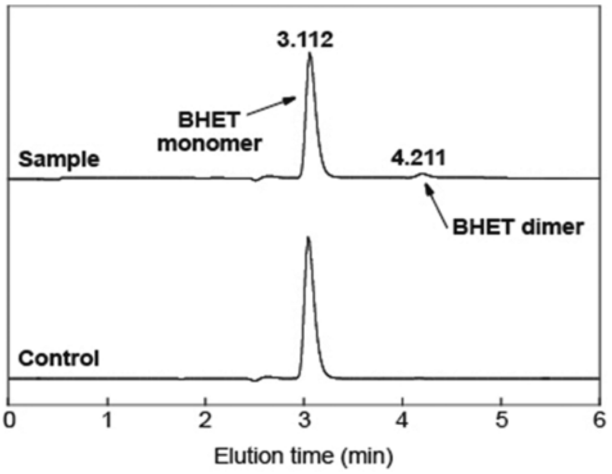

Fig. 10. HPLC chromatograms of BHET fractions from pretreated PET fabric samples and control.

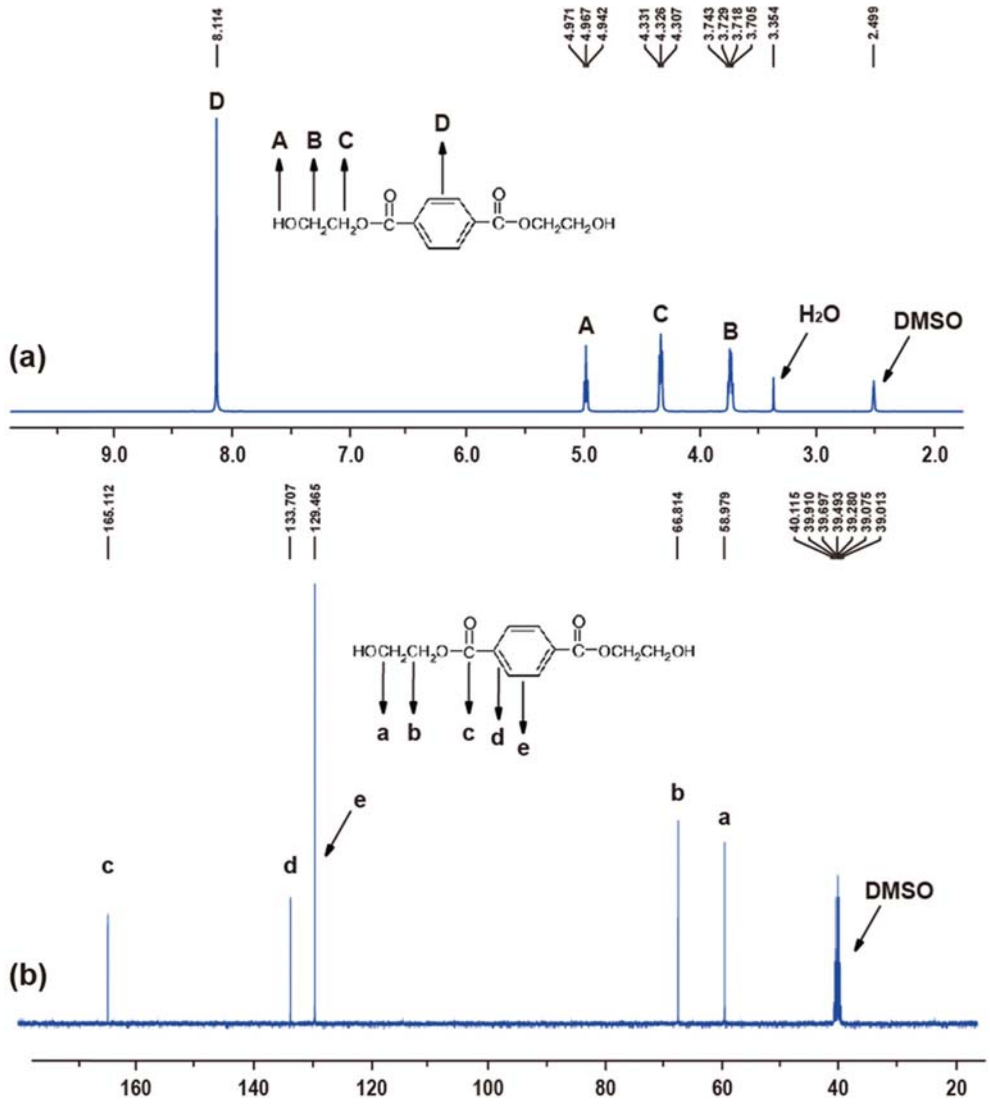

Fig. 11. NMR spectra of separated BHET monomer (a) ^{1}H-NMR of BHET monomer and (b) ^{13}C NMR of BHET monomer.

ous studies [36,37].

The BHET sample was further investigated by HPLC. Fig. 10 shows the HPLC chromatogram of BHET sample and control. The results show one dominant peak at the retention time of 3.112 minutes, which indicates the separation of BHET monomer. A tiny peak occurred at 4.211 minutes, which is associated with BHET dimer [4].

Chemical structure of the BHET monomer was analyzed by nuclear magnetic resonance (NMR) spectroscopy. The ^{1}H-NMR, and ^{13}C-NMR of the BHET monomer are shown in Fig. 11. The proton (Fig. 11(a)) and carbon (Fig. 11(b)) spectra of the BHET indicate that the monomer produced by the glycolysis is almost pure BHET. The peaks labelled A, B, C, and D (Fig. 11(a)) show the resonance of the protons of the outer hydroxyl groups (δ_H=4.9 ppm), methylenes (-CH$_2$-) near the outer -OH groups (δ_H=3.7ppm), methylenes (-CH$_2$-) near the -COO- groups (δ_H=4.3 ppm), and aromatic benzene group (δ_H=8.1 ppm, respectively. The peaks a (δ_C=58.9 ppm), b (δ_C=66.8 ppm), c (δ_C=165.1 ppm), d (δ_C=133.7 ppm), and e (δ_C= 129.4 ppm) correspond to the backbone carbon of the chemical structure of BHET monomer, as shown in Fig. 11(b). The peaks of DMSO and H$_2$O account for solvent and water contamination in the sample.

The observation of no secondary peaks in the NMR spectra indicates the high purity of BHET monomer. The NMR spectra of the BHET monomer are in very good agreement with the previous studies [36-39]. The thermal analysis and chemical structure analysis verified that the BHET monomer produced via this process had a high level of purity due to good monomer separation from the glycolysis reaction products.

5. Proposed Pretreatment Mechanism

Based on our results d in this study, a pretreatment mechanism is proposed and shown in Fig. 12. Silica particles are dissolved in NaOH solution to form various silicate anions during the pretreatment. Coating layer of silica-coated PET fabrics is destroyed so that dyes, unreacted silica particles, and other impurity can be easily detached from the fabrics.

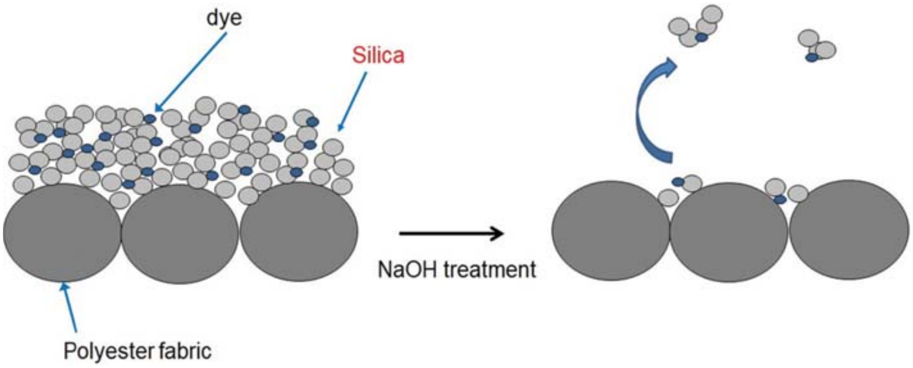

Fig. 12. Pretreatment mechanism of silica-coated PET fabrics using NaOH solution.

CONCLUSIONS

NaOH pretreatment successfully removed the impurities of the silica-coated PET fabric samples prior to glycolysis. The structure of silica coating layer was successfully degraded and removed from the PET fabric samples, which was confirmed through various analyses, including XPS, SEM, and EDX. The BHET yield was significantly improved by the pretreatment, and purity of the BHET monomer was confirmed by DSC, TGA, HPLC and NMR analyses. A potential possibility of the pretreatment of the low-grade PET wastes was verified. It showed great impurity removal performance resulting in higher BHET yield compared to untreated low-grade PET wastes. Therefore, this method will meet the current needs of process for impurity removal from PET wastes for further application.

ACKNOWLEDGEMENTS

This study was supported by the R&D Center for Valuable Recycling (Global-Top R&BD Program) of the Ministry of Environment (Project No.: 2016002240001).

REFERENCES

1. Q. Wang, X. Yao, Y. Geng, Q. Zhou, X. Lu and S. Zhang, *Green Chem.*, **17**, 2473 (2015).
2. S. H. Park and S. H. Kim, *Fash. Text.*, **1**, 22 (2014).
3. R. Shamsi and G. M. M. Sadeghi, *RSC Adv.*, **6**, 38399 (2016).
4. M. Imran, D. H. Kim, W. A. Al-Masry, A. Mahmood, A. Hassan, S. Haider and S. M. Ramay, *Polym. Degrad. Stab.*, **98**, 904 (2013).
5. S. R. Tharmapuram and S. A. Jabarin, *Adv. Polym. Technol.*, **2**, 147 (2003).
6. S. R. Tharmapuram and S. A. Jabarin, *Adv. Polym. Technol.*, **2**, 155 (2003).
7. D. E. Nikles and M. S. Farahat, *Macromol. Mater. Eng.*, **290**, 13 (2005).
8. S. C. Lee, Y. W. Sze and C. C. Lin, *J. Appl. Polym. Sci.*, **55**, 1271 (1995).
9. M. Li, Y. Huang, T. Yu, S. Chen, A. Ju and M. Ge, *RSC Adv.*, **4**, 46476 (2014).
10. P. K. George, K. N. Alexandros, D. S. Irini, N. B. Dimitris and S. A. Dimitris, *Macromol. Mater. Eng.*, **291**, 1338 (2006).
11. L. Bartolome, M. Imran, K. G. Lee, A. Sangalang, J. K. Ahn and D. H. Kim, *Green Chem.*, **16**, 279 (2014).
12. A. M. Al-Sabagh, F. Z. Yehia, D. R. K. Harding, G. Eshaq and A. E. ElMetwally, *Green Chem.*, **18**, 3997 (2016).
13. G. Park, L. Bartolome, K. G. Lee, S. J. Lee, D. H. Kim and T. J. Park, *Nanoscale*, **4**, 3879 (2012).
14. P. G. Demertzis, F. Johansson, C. Lievens and R. Franz, *Packag. Technol. Sci.*, **10**, 45 (1997).
15. S. Gupta, *Indian J. Fibre Text. Res.*, **26**, 156 (2001).
16. Q. Fan, Y. K. Kim, M. K. Perruzzi and A. F. Lewis, *J. Imaging Sci. Technol.*, **47**, 400 (2003).
17. X. Wu, Y. Wang, W. Yang, B. Xie, M. Yang and W. Dan, *Soft Matter*, **8**, 10457 (2012).
18. V. M. Gun'ko, I. F. Mironyuk, V. I. Zarko, V. V. Turv, E. F. Voronin, E. M. Pakhlov, E. V. Goncharuk, R. Leboda, J. Skubiszewska-Zieba, W. Janusz, S. Chibowski, Y. N. Levchuk and A. V. Klyuevaz, *J. Colloid Interface Sci.*, **242**, 90 (2001).
19. J. Nordstrom, A. Matic, J. Sun, M. Forsyth and D. R. MacFarlane, *Soft Matter*, **6**, 2293 (2010).
20. S. Kim, J. H. Sung, K. H. Ahn and S. J. Lee, *Langmuir*, **25**, 6155 (2009).
21. T. Lamminmaki, E. Kentta, H. Rautkoski, J. Bacher, S. Teir, J. Kettle and J. Sarlin, *J. Surf. Eng. Mater. Adv. Technol.*, **3**, 224 (2013).
22. Y. J. Wu, V. Lovell, A. Pekarovicova, P. D Fleming and M. Joyce, *J. Graphic Technol.*, **6**, 6 (2013).
23. M. Fertani-Gmati, K. Brahim, I. Khattech and M. Jemal, *Thermochim. Acta*, **594**, 58 (2014).
24. S. A. Greenberg, *J. Phys. Chem.*, **61**, 960 (1957).
25. C. J. Brinker, *J. Non. Cryst. Solids*, **100**, 31 (1988).
26. A. M. Al-Sabagh, F. Z. Yehia, Gh. Eshaq, A. M. Rabie and A. E. ElMetwall, *Egypt J. Petroleum*, **25**, 53 (2016).
27. G. P. Karayannidis and D. S. Achilias, *Macromol. Mater. Eng.*, **292**, 128 (2007).
28. R. Lopez-Fonseca, I. Duque-Ingunza, B. Rivas, S. Arnaiz and J. I. Gutierrez-Ortiz, *Polym. Degrad. Stab.*, **95**, 1022 (2010).
29. L. Bartolome, M. Imran, B. G. Cho, W. A. Al-Masry and D. H. Kim, In: D. Achilias, Ed., *Material Recycling - Trends and Perspectives*, ISBN: 978-953-51-0327-1, InTech (2012).
30. G. Xi, M. Lu and C. Sun, *Polym. Degrad. Stab.*, **87**, 117 (2004).
31. S. Fakirov, In: O. Olabisi, ed. *Handbook of thermoplastics*, CRC Press, 449 (1994).

32. Y. B. Ryu and M. S. Lee, *Korean J. Met. Mater.*, **56**, 72 (2018).
33. Q. W. Chen, X. G. Li, Y. H. Zhang and Y. T. Qian, *Adv. Mater.*, **25**, 134 (2002).
34. M. M. Mahmoud, D. C. Folz, C. T. A. Suchicital and D. E. Clark, *J. Am. Ceram. Soc.*, **95**, 95 (2012).
35. F. Jendoubi, A. Mgaidi and M. E. Maaoui, *Can. J. Chem. Eng.*, **75**, 721 (1997).
36. A. M. Al-Sabagh, F. Z. Yehia, A. M. F. Eissa, M. E. Moustafa, Gh. Eshaq and A. M. Rabie, *Polym. Degrad. Stab.*, **110**, 364 (2014).
37. H. Wang, Y. Liu, Z. Li, X. Zhang, S. Zhang and Y. Zhang, *Eur. Polym. J.*, **45**, 1535 (2009).
38. Q. F. Yue, C. X. Wang, L. N. Zhang, Y. Ni and Y. X. Jin, *Polym. Degrad. Stab.*, **96**, 399 (2011).
39. M. R. Nabid, Y. Bide, N. Fereidouni and B. Etemadi, *Polym. Degrad. Stab.*, **144**, 434 (2017).